

PUBLISHED VERSION

Wang, P.; Leinweber, Derek Bruce; Thomas, Anthony William; Young, Ross Daniel
[Strange magnetic form factor of the proton at \$Q^2=0.23 \text{ GeV}^2\$](#) Physical Review C, 2009;
79(6):065202

© 2009 American Physical Society

<http://link.aps.org/doi/10.1103/PhysRevC.79.065202>

PERMISSIONS

<http://publish.aps.org/authors/transfer-of-copyright-agreement>

“The author(s), and in the case of a Work Made For Hire, as defined in the U.S. Copyright Act, 17 U.S.C.

§101, the employer named [below], shall have the following rights (the “Author Rights”):

[...]

3. The right to use all or part of the Article, including the APS-prepared version without revision or modification, on the author(s)' web home page or employer's website and to make copies of all or part of the Article, including the APS-prepared version without revision or modification, for the author(s)' and/or the employer's use for educational or research purposes.”

27th March 2013

<http://hdl.handle.net/2440/56496>

Strange magnetic form factor of the proton at $Q^2 = 0.23 \text{ GeV}^2$

P. Wang,¹ D. B. Leinweber,² A. W. Thomas,^{1,3} and R. D. Young⁴

¹*Jefferson Laboratory, 12000 Jefferson Avenue, Newport News, Virginia 23606, USA*

²*Special Research Center for the Subatomic Structure of Matter (CSSM) and Department of Physics, University of Adelaide, Adelaide, SA 5005, Australia*

³*Department of Physics, College of William and Mary, Williamsburg, Virginia 23187, USA*

⁴*Physics Division, Argonne National Laboratory, Argonne, Illinois 60439, USA*

(Received 22 December 2008; published 9 June 2009)

We determine the u and d quark contributions to the proton magnetic form factor at finite momentum transfer by applying chiral corrections to quenched lattice data. Heavy baryon chiral perturbation theory is applied at next-to-leading order in the quenched and full QCD cases for the valence sector using finite range regularization. Under the assumption of charge symmetry these values can be combined with the experimental values of the proton and neutron magnetic form factors to deduce a relatively accurate value for the strange magnetic form factor at $Q^2 = 0.23 \text{ GeV}^2$, namely, $G_M^s = -0.034 \pm 0.021 \mu_N$.

DOI: 10.1103/PhysRevC.79.065202

PACS number(s): 14.20.Dh, 13.40.-f, 12.39.Fe, 11.10.Gh

Strange quark contributions to the properties of the nucleon have attracted a lot of interest since the originally puzzling European Muon Collaboration results concerning the proton spin [1]. Although that motivation has faded [2,3], it remains a central issue in QCD, especially with respect to lattice QCD, where such terms necessarily involve so-called “disconnected graphs,” i.e., quark loops that are connected only by gluon lines to the valence quarks. Despite enormous effort [4], the *direct* lattice calculations of these contributions have so far been unable to produce a result that differs statistically from zero. However, by using the constraints of charge symmetry, which is expected to be accurate at the 1% level or better [5,6], one can write relations [cf. Eqs. (17) and (18), below] for the disconnected contributions to physical form factors [7] in terms of valence quantities, which *can* be accurately calculated in lattice QCD, and the experimentally determined form factors. In the case of the strange magnetic moment and charge radius of the proton, this approach has succeeded admirably [8,9]. Here we apply the technique to the strange magnetic form factor at $Q^2 = 0.23 \text{ GeV}^2$.

Parity-violating electron scattering (PVES) has proven to be a valuable tool for experimentally determining the strange quark contribution to the electromagnetic form factors of the proton. Under the assumption of charge symmetry, one can deduce the strange electric or magnetic form factor ($G_{E,M}^s(Q^2)$) from measurements of the corresponding proton and neutron electromagnetic form factors *and* the neutral-weak vector form factor of the proton, through its contribution to PVES. While PVES measurements are very challenging, a number of groups have succeeded, starting with SAMPLE at Bates [10] and then A4 at Mainz [11] and G0 [12] and HAPPEX [13–15] at Jefferson Lab. A global analysis of all this data has given very precise values for the strange quark contribution to the proton magnetic moment, as well as its charge radius [16], which are consistent with the theoretical calculations mentioned above. The motivation for our current work is the knowledge that in the near future we expect new measurements from A4 and G0 at $Q^2 = 0.23 \text{ GeV}^2$.

In addition to the extensive experimental activity, a variety of theoretical models have been applied to the calculation of the strange nucleon form factors. These approaches include the QCD equalities supplemented with constituent quark model assumptions [17], heavy baryon chiral perturbation theory [18,19], dispersive approaches [20–22], the vector dominance model (VDM) [23], the VDM with a kaon cloud contribution [24], the Skyrme model [25], the NJL model [26], the chiral soliton [27,28], chiral bag [29] and chiral quark models [30–32], a two-component model with a meson cloud [33], etc. These theoretical predictions vary quite widely. For example, the predicted strange magnetic moment varies from relatively large and negative, -0.75 ± 0.30 [17] to sizably positive, $+0.37$ [29].

As well as the above model calculations, there have been some lattice simulations of the strange magnetic moment, with early lattice simulations giving a relatively large negative value [7,34,35]. In 2003, Lewis *et al.* [4] used low order, quenched chiral perturbation theory together with the lattice QCD simulation to calculate the strange form factors from lattice data. The magnetic form factor that they obtained at $Q^2 = 0.1 \text{ GeV}^2$ was $+0.05 \pm 0.06$. Recently, by combining the constraints of charge symmetry with new chiral extrapolation techniques and low mass, quenched lattice QCD simulations of the individual quark contributions to the magnetic moments of the nucleon octet, a precise, nonzero value, $G_M^s(0) = -0.046 \pm 0.019$, was obtained [8].

In this article, we present the lattice prediction for the strange magnetic form factor at $Q^2 = 0.23 \text{ GeV}^2$. We first extrapolate the u and d quark contributions to the proton magnetic form factor in quenched, heavy baryon chiral perturbation theory [36,37]. The quenched lattice data from the CSSM Lattice Collaboration are used and finite-range regularization (FRR) is applied in the extrapolation, because of its improved convergence behavior at intermediate and large quark mass [38–42]. In the following we briefly introduce the chiral Lagrangian that is used in the extrapolation. The formal calculation of the magnetic form factor is then explained, followed by the numerical results.

There are many articles that deal with heavy baryon chiral perturbation theory. For details see, for example, Refs. [43–45]. For completeness, we briefly introduce the formalism here. In the heavy baryon chiral perturbation theory, the lowest order chiral Lagrangian for the baryon-meson interaction, which will be used in the calculation of the electromagnetic magnetic form factors, including the octet and decuplet baryons, is expressed as

$$\begin{aligned} \mathcal{L}_v = & i\text{Tr}\bar{B}_v(v \cdot D)B_v + 2D\text{Tr}\bar{B}_v S_v^\mu \{A_\mu, B_v\} \\ & + 2F\text{Tr}\bar{B}_v S_v^\mu [A_\mu, B_v] - i\bar{T}_v^\mu (v \cdot D)T_{v\mu} \\ & + C(\bar{T}_v^\mu A_\mu B_v + \bar{B}_v A_\mu T_v^\mu), \end{aligned} \quad (1)$$

where S_μ is the covariant spin-operator, defined as

$$S_v^\mu = \frac{i}{2}\gamma^5\sigma^{\mu\nu}v_\nu. \quad (2)$$

Here, v^ν is the nucleon four velocity [in the rest frame, we have $v^\nu = (1, 0)$]. D , F , and C are the coupling constants. The chiral covariant derivative, D_μ , is written as $D_\mu B_v = \partial_\mu B_v + [V_\mu, B_v]$. The pseudoscalar meson octet couples to the baryon field through the vector and axial vector combinations

$$V_\mu = \frac{1}{2}(\zeta\partial_\mu\zeta^\dagger + \zeta^\dagger\partial_\mu\zeta), \quad A_\mu = \frac{1}{2}(\zeta\partial_\mu\zeta^\dagger - \zeta^\dagger\partial_\mu\zeta), \quad (3)$$

where

$$\zeta = e^{i\phi/f}, \quad f = 93 \text{ MeV}. \quad (4)$$

The matrix of pseudoscalar fields, ϕ , is expressed as

$$\phi = \frac{1}{\sqrt{2}} \begin{pmatrix} \frac{1}{\sqrt{2}}\pi^0 + \frac{1}{\sqrt{6}}\eta & \pi^+ & K^+ \\ \pi^- & -\frac{1}{\sqrt{2}}\pi^0 + \frac{1}{\sqrt{6}}\eta & K^0 \\ K^- & \bar{K}^0 & -\frac{2}{\sqrt{6}}\eta \end{pmatrix}. \quad (5)$$

B_v and T_v^μ are the velocity-dependent new fields, which are related to the original baryon octet and decuplet fields, B and T^μ , by

$$B_v(x) = e^{im_N v^\nu x^\nu} B(x), \quad (6)$$

$$T_v^\mu(x) = e^{im_N v^\nu x^\nu} T^\mu(x). \quad (7)$$

In the chiral SU(3) limit, the octet baryons are degenerate. In our calculation we use the physical mass splittings for transition meson-baryon loop diagrams.

In the heavy baryon formalism, the propagators of the octet or decuplet baryon, j , are expressed as

$$\frac{i}{v \cdot k - \Delta + i\varepsilon} \quad \text{and} \quad \frac{iP^{\mu\nu}}{v \cdot k - \Delta + i\varepsilon}, \quad (8)$$

where $P^{\mu\nu}$ is $v^\mu v^\nu - g^{\mu\nu} - (4/3)S_v^\mu S_v^\nu$ and $\Delta = m_j - m_N$ is the mass difference between the baryon j and the nucleon. The propagator of meson j ($j = \pi, K, \eta$) is the usual free

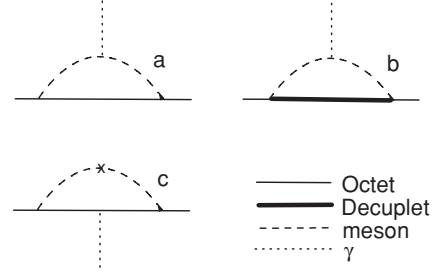


FIG. 1. Leading and next-to-leading order diagrams for the proton magnetic form factors. The last diagram, c, need only be included in the quenched case.

propagator:

$$\frac{i}{k^2 - M_j^2 + i\varepsilon}. \quad (9)$$

In the heavy baryon formalism, the electromagnetic form factors are defined as

$$\begin{aligned} \langle B(p') | J_\mu | B(p) \rangle = & \bar{u}(p') \left\{ v_\mu G_E(Q^2) \right. \\ & \left. + \frac{i\epsilon_{\mu\nu\alpha\beta} v^\alpha S_v^\beta q^\nu}{m_N} G_M(Q^2) \right\} u(p), \end{aligned} \quad (10)$$

where J_μ is the charge current, $q = p' - p$, and $Q^2 = -q^2$. In this article, we focus on the magnetic form factors in each quark sector, aiming to extract the strange quark contribution.

With the Lagrangian given earlier, the leading and next-to-leading order diagrams for the magnetic form factor are shown in Fig. 1. In full QCD, the first diagram, a, is the leading diagram, while diagram b gives the next-to-leading order nonanalytic term, because of the mass difference between octet and decuplet baryons. The last, or so-called double hairpin, diagram need be considered only for the quenched case, where the η' is degenerate with the pion.

The contribution to the magnetic form factor of Fig. 1(a) is expressed as

$$G_M^a(Q^2) = \frac{-M_N \beta^a}{8\pi^3 f_\pi^2} \int d^3k \frac{k_y^2 u(\vec{k} + \vec{q}/2) u(\vec{k} - \vec{q}/2)}{\omega(\vec{k} + \vec{q}/2)^2 \omega(\vec{k} - \vec{q}/2)^2}. \quad (11)$$

$\omega_j(\vec{k}) = \sqrt{m_j^2 + \vec{k}^2}$ is the energy of the meson j . We regulate the loop integral using finite range regularization, with $u(\vec{k})$ being the ultraviolet regulator. Both the pion and kaon are included in the calculation. In full QCD, the coefficients are obtained from the Lagrangian. In the quenched case the coefficients are obtained as in Refs. [36,44,46].

The contribution to the magnetic form factor of Fig. 1(b) can be written as

$$G_M^b(Q^2) = \frac{-M_N \beta^b}{8\pi^3 f_\pi^2} \int d^3k \frac{k_y^2 u(\vec{k} + \vec{q}/2) u(\vec{k} - \vec{q}/2) (\omega(\vec{k} + \vec{q}/2) + \omega(\vec{k} - \vec{q}/2))}{A}, \quad (12)$$

TABLE I. Coefficients, β^a , for quarks in quenched, valence, and full QCD for Fig. 1(a). The left three columns are for an intermediate π meson and the right three columns are for an intermediate K meson.

Quark	u	d	s	u	d	s
Quench	$-\frac{4}{3}D^2$	$\frac{4}{3}D^2$	0	0	0	0
Valence	$-4F^2 - \frac{8}{3}D^2$	$-\frac{2}{3}D^2 + 4DF - 2F^2$	0	$-\frac{1}{6}(3F + D)^2 \Lambda K$	$-(D - F)^2$	0
Full QCD	$-(D + F)^2$	$(D + F)^2$	0	$-\frac{1}{2}(D - F)^2 \Sigma K$	$-(D - F)^2$	$\frac{1}{6}(3F + D)^2 \Lambda K$
				$-\frac{1}{6}(3F + D)^2 \Lambda K$		$\frac{3}{2}(D - F)^2 \Sigma K$

where

$$A = \omega(\vec{k} + \vec{q}/2)\omega(\vec{k} - \vec{q}/2)(\omega(\vec{k} + \vec{q}/2) + \Delta) \times (\omega(\vec{k} - \vec{q}/2) + \Delta)(\omega(\vec{k} + \vec{q}/2) + \omega(\vec{k} - \vec{q}/2)). \quad (13)$$

In the preceding equations, β^i ($i = a, b$) depends on the quark type, the meson loop type, and whether the calculation involves quenched or full QCD in the calculation.

In the quenched case, the additional double hairpin term from the η' is expressed as

$$G_M^c(Q^2) = \frac{(3F - D)^2 M_0^2 G_M(Q^2)}{288\pi^3 f_\pi^2} \int d^3k \frac{\vec{k}^2 u(\vec{k})^2}{\omega(\vec{k})^5}, \quad (14)$$

where M_0 is the double hairpin interaction strength. We note that the integral of Eq. (14) gives rise to a logarithmic divergence in the chiral limit. As a result we estimate the contribution of this graph using the renormalized value of $G_M(Q^2)$ obtained from the lattice simulation results at finite quark-mass values. Of course, in full QCD no such term needs to be included.

In the above formulas, the coefficients in quenched, valence, and full QCD can be obtained with the same method as used in Ref. [46]. For example, Fig. 1(a) is shown in detail in terms of the underlying quark lines in Fig. 2. In quenched QCD, the diagram with a quark loop has no contribution. In the case of the valence quark sector, as well as the quenched diagram, the diagram with a quark loop can also have a contribution if the external photon field couples to the valence quark. In full QCD, both the valence quark and the sea quark (loop) couple to the photon field. For the pion loop, in full QCD, Figs. 2(a) and 2(c) give contributions, while in the quenched case, Figs. 2(a) and 2(b) give contributions. The coefficients for Figs. 2(c) and 2(i) are the same as those for Fig. 2(e), which are known from

 TABLE II. Coefficients, β^b , for quarks in quenched, valence, and full QCD for Fig. 1(b). The left three columns are for an intermediate π meson and the right three columns are for an intermediate K meson.

Quark	u	d	s	u	d	s
Quench	$-\frac{c^2}{6}$	$\frac{c^2}{6}$	0	0	0	0
Valence	$-\frac{c^2}{18}$	$\frac{7c^2}{18}$	0	$\frac{c^2}{18}$	$\frac{c^2}{9}$	0
Full QCD	$-\frac{2c^2}{9}$	$\frac{2c^2}{9}$	0	$\frac{c^2}{18}$	$\frac{c^2}{9}$	$-\frac{c^2}{6}$

the Lagrangian, because QCD is flavor blind. For the same reason, the coefficients for Figs. 2(d) and 2(h) are the same as those for Fig. 2(f). By subtracting the known coefficients from the total coefficients of full QCD, we can get the coefficients for each diagram in Fig. 2. The resulting coefficients for each quark for the different cases are summarized in Tables I and II.

As we know, most detailed lattice simulations for the nucleon electromagnetic form factors have been computed in the quenched approximation, in which the strange magnetic form factor is identically zero. Because the value in full QCD is not large, any direct calculation of G_M^s will require considerable effort to extract an accurate value. In this article, we first concentrate on computing the contribution of each valence quark to the proton form factor, in the physical theory at the physical mass. Then by using charge symmetry and the experimental proton and neutron form factors, we are able to extract a precise value of the strange magnetic form factor using the techniques of Refs. [7] and [8].

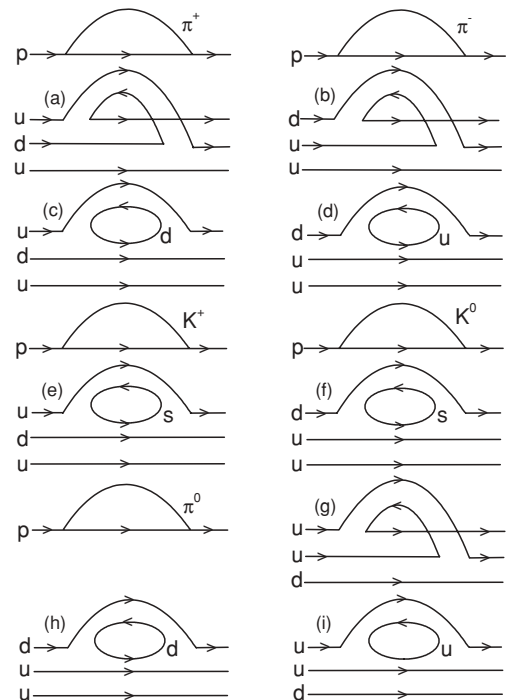


FIG. 2. Feynman diagrams at the quark level, which are included in Fig. 1(a) for the proton magnetic form factor.

The magnetic form factor can be expressed as

$$G_M(Q^2) = a_0 + a_2 m_\pi^2 + a_4 m_\pi^4 + \sum_{i=a}^c G_M^i(Q^2), \quad (15)$$

where the parameters a_0 , a_2 , and a_4 can be obtained by fitting the quenched lattice data. In the numerical calculations, the SU(3) parameters are chosen to be $D = 0.76$ and $F = 0.50$ ($g_A = D + F = 1.26$) and the coupling constant C is $-2D$. The FRR regulator, or form factor, $u(k)$, is taken to be a dipole ($u(k) = \frac{1}{(1+k^2/\Lambda^2)^2}$, with $\Lambda = 0.8$ GeV), although as shown by Young *et al.* [41] the model dependence associated with other choices is small.

We use SU(2) chiral symmetry, with only the light quark masses varying and the strange quark mass fixed. Thus the K -meson mass is related to the pion mass by

$$m_K^2 = \frac{1}{2} m_\pi^2 + m_K^2|_{\text{phy}} - \frac{1}{2} m_\pi^2|_{\text{phy}}, \quad (16)$$

which enables a direct relationship between the meson dressings of the magnetic form factor and the pion mass.

The contribution of a single u quark with unit charge to the proton magnetic form factor is shown in Fig. 3. The dotted, dashed, and solid lines are for the quenched, valence sector, and full QCD results, respectively. The square points with error bars are the quenched lattice data obtained by the CSSM Lattice Collaboration [47]. The lattice results were fit with finite volume chiral perturbation theory followed by corrections to yield the infinite volume results. The FRR quenched chiral perturbation theory describes the lattice data results well over the range $m_\pi^2 \in 0.1-0.7$ GeV². At the physical pion mass, the quenched (${}^q G_M^u$), valence (${}^v G_M^u$), and full QCD (${}^f G_M^u$) values of the magnetic form factor are 1.099 ± 0.165 , 1.221 ± 0.183 , and 1.179 ± 0.177 , respectively.

In Fig. 4, we show the contribution of the d quark, with unit charge, to the proton magnetic form factor. The three styles of line have the same meaning as described in Fig. 3.

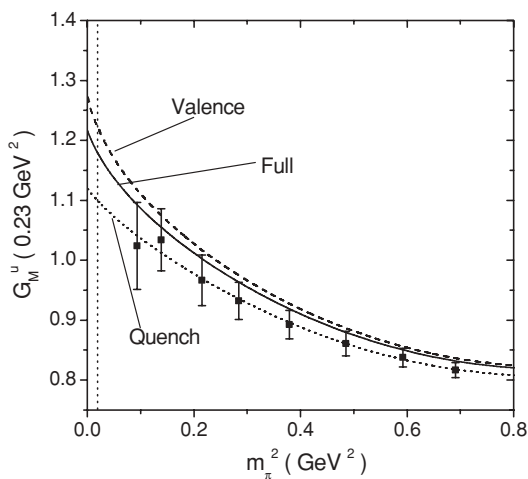


FIG. 3. The contribution of a single u quark, with unit charge, to the proton magnetic form factor at $Q^2 = 0.23$ GeV² versus pion mass. The dotted, dashed, and solid lines denote the quenched (finite volume), valence sector, and full QCD (infinite volume) results, respectively.

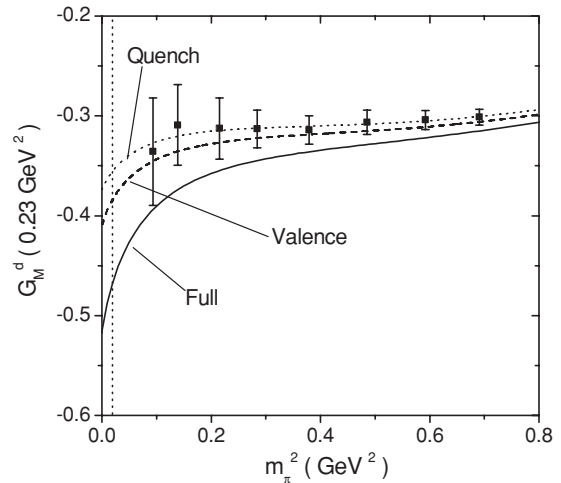


FIG. 4. The contribution of a d quark, with unit charge, to the proton magnetic form factor at $Q^2 = 0.23$ GeV² versus pion mass. The dotted, dashed, and solid lines denote the quenched (finite volume), valence sector, and full QCD (infinite volume) results, respectively.

Again, the quenched lattice results are described very well. In contrast with the u quark case, the absolute value of the d quark contribution in full QCD is larger than that in the valence case. This is consistent with the disconnected contribution and hence the strange quark form factor being small and negative. At the physical pion mass, the quenched (${}^q G_M^d$), valence (${}^v G_M^d$), and full QCD (${}^f G_M^d$) values of the d quark contribution are -0.356 ± 0.053 , -0.383 ± 0.057 , and -0.468 ± 0.070 , respectively.

With the full QCD values of the u and d quark contributions, one can get the strange form factor by subtracting them from the proton or neutron magnetic form factor. However, because of the small value of G_M^s , the error bar obtained in this direct calculation is much larger than the central value of G_M^s . We therefore use the valence contributions ${}^v G_M^u$ and ${}^v G_M^d$, which yield a relatively precise value of G_M^s .

The proton and neutron magnetic form factors can be written in terms of quark components as [7]

$$G_M^p = \frac{4}{3} {}^v G_M^u - \frac{1}{3} {}^v G_M^d + {}^l O_M^p, \quad (17)$$

$$G_M^n = \frac{2}{3} {}^v G_M^d - \frac{2}{3} {}^v G_M^u + {}^l O_M^n, \quad (18)$$

where ${}^l O_M^p = {}^l O_M^n = \frac{2}{3} {}^l G_M^u - \frac{1}{3} {}^l G_M^d - \frac{1}{3} G_M^s$. The label l denotes a “loop” or sea quark contribution, while the label v means a connected valence quark contribution in full QCD. In the equations above, charge symmetry has been used; i.e., the u and d quark contributions in the proton are the same as the corresponding d and u quark contributions in the neutron. Charge symmetry is known to be accurate at better than 1% where it has been tested, primarily in nuclear systems. It must be assumed to extract the strange form factors from parity-violating electron scattering. Under the assumption of charge symmetry, the strange quark contribution in the proton is the same as that in the neutron.

The contribution from the quark in the loop in Fig. 2 depends *only* on its mass; i.e., it is independent of whether the

quark in the loop is labeled u , d , or s . The loop contribution of each quark can be obtained using Eqs. (11) and (12) with the same coefficients $\frac{5}{3}D^2 - 2DF + 3F^2$ and $-\frac{C^2}{6}$. By calculation of the relevant loops using FRR, we evaluate the ratio ${}^l R_d^s = G_M^s / {}^l G_M^d$ at $Q^2 = 0.23 \text{ GeV}^2$. This yields the value ${}^l R_d^s = 0.185 \pm 0.038$ allowing the dipole mass parameter to vary between 0.6 and 1.0 GeV. Then, using Eqs. (17) and (18), we find

$$G_M^s = \frac{{}^l R_d^s}{1 - {}^l R_d^s} (2G_M^p + G_M^n - 2{}^v G_M^u), \quad (19)$$

$$G_M^s = \frac{{}^l R_d^s}{1 - {}^l R_d^s} (G_M^p + 2G_M^n - {}^v G_M^d). \quad (20)$$

In Ref. [8], because we were working at $Q^2 = 0$, it was possible to use the measured magnetic moments of the nucleon and the hyperons. Because the hyperon magnetic form factors are not known at finite Q^2 , here we must use the extrapolated valence quark contributions (rather than ratios) to extract the strange form factor. The experimental values of $G_M^p(0.23)$ and $G_M^n(0.23)$ are $\frac{G_M^p(0.23)}{\mu_p G_D(0.23)} = 0.98 \pm 0.01$ [48] and $\frac{G_M^n(0.23)}{\mu_n G_D(0.23)} = 0.96 \pm 0.01$ [49], where G_D is the dipole function expressed as $G_D(Q^2) = 1/(1 + Q^2/0.71 \text{ GeV}^2)^2$. Substituting the experimental magnetic moment of the proton (2.793) and neutron (-1.913), we obtain the values $G_M^p(0.23) + 2G_M^n(0.23) = -0.534 \pm 0.036$ and $2G_M^p(0.23) + G_M^n(0.23) = 2.075 \pm 0.041$. Comparing the latter with twice the value of ${}^v G_M^u = 1.221 \pm 0.183$, obtained from our chiral analysis of the lattice results, it is clear that there is a significant cancellation in Eq. (19). Furthermore, the large value of $2{}^v G_M^u$ means that the corresponding error on $G_M^s(0.23)$ extracted from Eq. (19) will be large. Indeed, we find that Eq. (19) yields $G_M^s(0.23) = -0.083 \pm 0.092$. (Note that the quoted error bar arises from the errors in the lattice data, the experimental magnetic form factors, and finally the theoretical uncertainty associated with FRR, especially the variation of the mass parameter Λ .) On the other hand, the relatively small value of ${}^v G_M^d = -0.383 \pm 0.057$ means that we obtain a much more accurate value of $G_M^s(0.23)$ using Eq. (20), namely, $G_M^s(0.23) = -0.034 \pm 0.021$. We note that the two extracted values of G_M^s are consistent within their respective error bars and that the sign of both, negative, is consistent with the difference between the extrapolations of the single quark magnetic moments in the valence and full QCD cases in Figs. 3 and 4.

Some theoretical predictions for the strange magnetic form factor are shown in Fig. 5. These models give different values of G_M^s that are all within the current experimental error bars. As for the experimental values of G_M^s , using the same techniques as described in Ref. [16], we find

$$G_M^s(Q^2) = 0.044 + 0.93Q^2 \pm \sqrt{0.34 - 7.02Q^2 + 47.8Q^4}, \quad (21)$$

where Q^2 is in GeV^2 . This form, which is the result of a global analysis of all published data [50], is valid over the range $0 < Q^2 < 0.3 \text{ GeV}^2$.

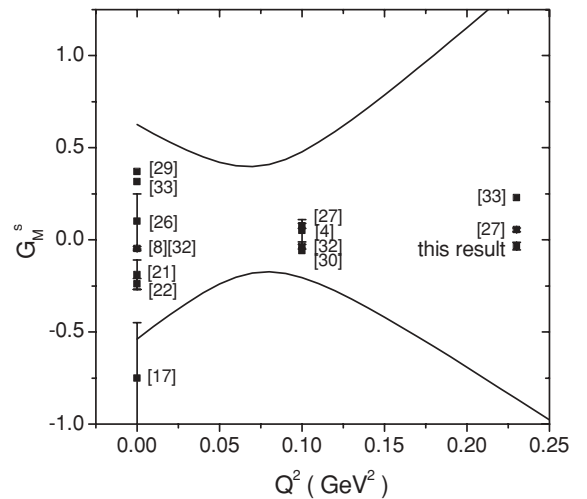


FIG. 5. Theoretical predictions of the strange magnetic form factors. The two lines are for the upper and lower limits of the experimental data with Eq. (21).

The issue of the errors in the strange magnetic moment was, of course, a serious issue in an earlier article [8], and there and in the companion articles [51,52] we explained all of the sources of error, including possible charge symmetry violation. The latter led to a much smaller contribution to the final error on G_M^s than the statistical errors on the lattice QCD data. This is also the case here at small but finite Q^2 . The dominance piece of the error, which we quote to $G_M^s(0.23)$, arises from the errors on the lattice determination of ${}^v G_M^d$ and the experimental errors on proton and neutron magnetic form factors, in comparison with which the errors expected from all that is known about charge symmetry breaking in nuclear physics, namely, that it is typically below 1%, really are negligible.¹

To conclude, we have extrapolated the lattice results for the separate valence quark contributions to the proton magnetic form factor at $Q^2 = 0.23 \text{ GeV}^2$ in quenched and full heavy baryon chiral perturbation theory. The leading and next-to-leading order diagrams are considered and all octet and decuplet baryons are included in the intermediate states. Finite-range regularization is used in the one loop calculation, both because it improves the convergence of the chiral expansion

¹We note that the size of the potential charge symmetry violation estimated in the calculation of Kubis and Lewis [53] is an exception, being an order of magnitude larger than that found in the earlier calculation by Miller *et al.* [5,54]. These authors used a very large anomalous ω - N coupling, in contrast with what we know from NN scattering. In addition, the ω coupling that they use (g_ω) is much larger than the usual one-boson exchange ω - N coupling. We also note that the implications of this work for other examples of charge symmetry violation have not yet been worked out. Nevertheless, if we were to use their extreme estimate, our result for $G_M^s(0.23)$ would change from -0.034 ± 0.021 to -0.025 ± 0.024 . The difference is very small and, in view of the concerns already noted, we prefer not to include this estimate of the charge symmetry correction in our final result.

and because it has been shown to permit a connection between quenched and dynamical lattice results [37]. By using the constraints of charge symmetry, we combine the extrapolated d valence quark contribution with the experimental proton and neutron magnetic form factors to obtain a surprisingly accurate determination of the strange magnetic form factor $G_M^s(0.23) = -0.034 \pm 0.021$. This is the first time it has proven possible to extract an accurate value of the strange magnetic form factor at $Q^2 = 0.23 \text{ GeV}^2$ using lattice QCD results. It will clearly be of considerable interest to compare this with the values that will be extracted from the recent A4 and G0 measurements at Mainz and JLab.²

ACKNOWLEDGMENTS

We thank the Australian Partnership for Advanced Computing (APAC) and eResearch South Australia for supercomputer support enabling this project. This work was authored by Jefferson Science Associates, LLC, under US DOE Contract DE-AC05-06OR23177. This work is supported by the Australian Research Council and by US DOE Contract DE-AC05-06OR23177, under which Jefferson Science Associates, LLC, operates Jefferson Laboratory, and Contract DE-AC02-06CH11357, under which UChicago Argonne, LLC, operates Argonne National Laboratory.

-
- [1] J. Ashman *et al.* (European Muon Collaboration), Phys. Lett. **B206**, 364 (1988).
- [2] F. Myhrer and A. W. Thomas, Phys. Lett. **B663**, 302 (2008).
- [3] A. W. Thomas, Prog. Part. Nucl. Phys. **61**, 219 (2008).
- [4] R. Lewis, W. Wilcox, and R. M. Woloshyn, Phys. Rev. D **67**, 013003 (2003).
- [5] G. A. Miller, Phys. Rev. C **57**, 1492 (1998).
- [6] G. A. Miller, B. M. K. Nefkens, and I. Slaus, Phys. Rep. **194**, 1 (1990).
- [7] D. B. Leinweber and A. W. Thomas, Phys. Rev. D **62**, 074505 (2000).
- [8] D. B. Leinweber *et al.*, Phys. Rev. Lett. **94**, 212001 (2005).
- [9] D. B. Leinweber *et al.*, Phys. Rev. Lett. **97**, 022001 (2006).
- [10] D. T. Spayde *et al.* (SAMPLE Collaboration), Phys. Lett. **B583**, 79 (2004).
- [11] F. E. Maas *et al.*, Phys. Rev. Lett. **94**, 152001 (2005).
- [12] D. S. Armstrong *et al.* (G0 Collaboration), Phys. Rev. Lett. **95**, 092001 (2005).
- [13] A. Acha *et al.* (HAPPEX Collaboration), Phys. Rev. Lett. **98**, 032301 (2007).
- [14] K. A. Aniol *et al.* (HAPPEX Collaboration), Phys. Lett. **B635**, 275 (2006).
- [15] K. A. Aniol *et al.* (HAPPEX Collaboration), Phys. Rev. C **69**, 065501 (2004).
- [16] R. D. Young, J. Roche, R. D. Carlini, and A. W. Thomas, Phys. Rev. Lett. **97**, 102002 (2006).
- [17] D. B. Leinweber, Phys. Rev. D **53**, 5115 (1996).
- [18] T. R. Hemmert, U. G. Meissner, and S. Steininger, Phys. Lett. **B437**, 184 (1998).
- [19] T. R. Hemmert, B. Kubis, and Ulf-G. Meissner, Phys. Rev. C **60**, 045501 (1999).
- [20] R. L. Jaffe, Phys. Lett. **B229**, 275 (1989).
- [21] H. Forkel, Phys. Rev. C **56**, 510 (1997).
- [22] H. W. Hammer, U. G. Meissner, and D. Drechsel, Phys. Lett. **B367**, 323 (1996).
- [23] S. Dubnicka, A. Z. Dubnickova, and P. Weisenpacher, arXiv:hep-ph/0102171.
- [24] T. D. Cohen, H. Forkel, and M. Nielsen, Phys. Lett. **B316**, 1 (1993).
- [25] N. W. Park, J. Schechter, and H. Weigel, Phys. Rev. D **43**, 869 (1991).
- [26] H. Weigel, A. Abada, R. Alkofer, and H. Reinhardt, Phys. Lett. **B353**, 20 (1995).
- [27] A. Silva, H. C. Kim, and K. Goetze, Phys. Rev. D **65**, 014016 (2001); **66**, 039902(E) (2002).
- [28] K. Goetze, H. C. Kim, A. Silva, and D. Urbano, Eur. Phys. J. A **32**, 393 (2007).
- [29] S. T. Hong, B. Y. Park, and D. P. Min, Phys. Lett. **B414**, 229 (1997).
- [30] L. Hannelius, D. O. Riska, and L. Y. Glozman, Nucl. Phys. **A665**, 353 (2000).
- [31] L. Hannelius and D. O. Riska, Phys. Rev. C **62**, 045204 (2000).
- [32] V. E. Lyubovitskij, P. Wang, T. Gutsche, and A. Faessler, Phys. Rev. C **66**, 055204 (2002).
- [33] R. Bijker, Rev. Mex. Fis. **S52N4**, 1 (2006).
- [34] S. J. Dong, K. F. Liu, and A. G. Williams, Phys. Rev. D **58**, 074504 (1998).
- [35] N. Mathur and S. J. Dong, Nucl. Phys. Proc. Suppl. **94**, 311 (2001).
- [36] S. R. Sharpe, Phys. Rev. D **46**, 3146 (1992).
- [37] R. D. Young, D. B. Leinweber, A. W. Thomas, and S. V. Wright, Phys. Rev. D **66**, 094507 (2002).
- [38] D. B. Leinweber, A. W. Thomas, and R. D. Young, Phys. Rev. Lett. **92**, 242002 (2004).
- [39] W. Armour, C. R. Allton, D. B. Leinweber, A. W. Thomas, and R. D. Young, J. Phys. G: Nucl. Part. Phys. **32**, 971 (2006).
- [40] C. R. Allton, W. Armour, D. B. Leinweber, A. W. Thomas, and R. D. Young, Phys. Lett. **B628**, 125 (2005).
- [41] R. D. Young, D. B. Leinweber, and A. W. Thomas, Prog. Part. Nucl. Phys. **50**, 399 (2003).
- [42] P. Wang, D. B. Leinweber, A. W. Thomas, and R. D. Young, Phys. Rev. D **75**, 073012 (2007).
- [43] E. E. Jenkins, M. E. Luke, A. V. Manohar, and M. J. Savage, Phys. Lett. **B302**, 482 (1993); **B388**, 866(E) (1996).
- [44] J. N. Labrenz and S. R. Sharpe, Phys. Rev. D **54**, 4595 (1996).
- [45] L. Durand, P. Ha, and G. Jaczko, Phys. Rev. D **64**, 014008 (2001).
- [46] D. B. Leinweber, Phys. Rev. D **69**, 014005 (2004).
- [47] S. Boinepalli, D. B. Leinweber, A. G. Williams, J. M. Zanotti, and J. B. Zhang, Phys. Rev. D **74**, 093005 (2006).

²The latest measurement of strange quark contribution to the vector form factors was reported after this article was submitted for publication [55]. The new result favors a negative strange magnetic form factor: $G_M^s(0.22 \text{ GeV}^2) = -0.14 \pm 0.11 \pm 0.11$.

- [48] A. Bodek, S. Avvakumov, R. Bradford, and H. Budd, *Eur. Phys. J. C* **53**, 349 (2008).
- [49] B. Anderson *et al.* (Jefferson Lab E95-001 Collaboration), *Phys. Rev. C* **75**, 034003 (2007).
- [50] R. D. Young, R. D. Carlini, A. W. Thomas, and J. Roche, *Phys. Rev. Lett.* **99**, 122003 (2007).
- [51] D. B. Leinweber, S. Boinepalli, A. W. Thomas, A. G. Williams, R. D. Young, J. B. Zhang, and J. M. Zanotti, *Eur. Phys. J. A* **24**, 79 (2005).
- [52] A. W. Thomas, R. D. Young, and D. B. Leinweber, in *Proceedings of the First Workshop on Quark-Hadron Duality and the Transition to pQCD, Frascati, 6–8 June 2005*, edited by A. Fantoni *et al.*, pp. 41–49.
- [53] B. Kubis and R. Lewis, *Phys. Rev. C* **74**, 015204 (2006).
- [54] G. A. Miller, A. K. Opper, and E. J. Stephenson, *Annu. Rev. Nucl. Part. Sci.* **56**, 253 (2006).
- [55] S. Baunack *et al.*, *Phys. Rev. Lett.* **102**, 151803 (2009).